Title	Microphthalmia-associated transcription factor is required for mature myotube formation.
Author(s)	Ooishi, Ryo; Shirai, Mitsuyuki; Funaba, Masayuki; Murakami, Masaru
Citation	Biochimica et biophysica acta (2012), 1820(2): 76-83
Issue Date	2012-02
URL	http://hdl.handle.net/2433/153284
Right	© 2011 Elsevier B.V.
Type	Journal Article
Textversion	author

Microphthalmia-associated transcription factor is required for mature myotube formation

Ryo Ooishi[1], Mitsuyuki Shirai[2], Masayuki Funaba[3,*] and Masaru Murakami[1,*]

[1]Laboratory of Molecular Biology, Azabu University School of Veterinary Medicine, Sagamihara 229-5201, Japan

[2]Laboratory of Veterinary Pharmacology, Azabu University School of Veterinary Medicine, Sagamihara 229-5201, Japan

[3]Division of Applied Biosciences, Kyoto University Graduate School of Agriculture, Kyoto 606-8502, Japan

Running title: Role of Mitf in myogenesis

*Correspondence:

Masayuki Funaba, Division of Applied Biosciences, Kyoto University Graduate School of Agriculture (mfunaba@kais.kyoto-u.ac.jp) or Masaru Murakami, Laboratory of Molecular Biology, Azabu University School of Veterinary Medicine (murakami@azabu-u.ac.jp)

Abstract

Background: The roles of microphthalmia-associated transcription factor (Mitf) in the skeletal muscle and during myogenesis are unclear.

Methods: Expression of *Mitf* in mouse tissues and during myogenesis was evaluated. Effects of *Mitf* knockdown on myogenesis and gene expression related to myogenesis were subsequently explored. Furthermore, effects of *p21*, a cyclin-dependent kinase inhibitor, and *integrin α9* (*Itga9*) were examined.

Results: Mitf was highly expressed in the skeletal muscle; *Mitf-A* and *-J* were expressed. Mitf expression increased after differentiation stimulation in C2C12 myogenic cells. Down-regulation of *Mitf* expression by transfection of siRNA for common *Mitf* inhibited myotube formation, which was reproduced by *Mitf-A* knockdown. Morphometric analyses indicated that both multinucleated cell number and the proportion of myotubes with more than 6 nuclei were decreased in *Mitf*-knockdown cells, suggesting that Mitf is required for not only the formation of nascent myotubes but also their maturation. Searching for genes positively regulated by Mitf revealed *p21* and *Itga9*; decreasing *Mitf* expression inhibited up-regulation of *p21* expression after differentiation stimulation and blocked the induction of *Itga9* expression in response to differentiation. Knockdown of *p21* decreased the number of multinucleated cells, whereas *Itga9* knockdown did not affect the myotube number. Both *p21* knockdown and *Itga9* knockdown decreased the proportion of myotubes with more than 6 nuclei.

Conclusion: The present study clarified that Mitf is significantly expressed during myogenesis, and that *Mitf* is required for efficient myotube formation through expression of p21 and Itga9.

General significance: Mitf positively regulates skeletal muscle formation.

Keywords: Mitf, myogenesis, integrin, p21, myotube

Introduction

Skeletal muscle formation consists of a complex set of differentiation steps: commitment of mesenchymal stem cells to myoblast lineage cells, progression of differentiation with the expression of muscle-cell-specific proteins, and fusion of myoblasts into multinucleated myotubes. Mammalian myotube formation occurs in two phases [1, 2]. In the first phase, differentiated myoblasts fuse together to form small myotubes; to accomplish this process, proliferating myoblasts exit cell cycle, and some myoblasts undergo apoptosis. In the second phase, additional myoblasts subsequently fuse with myotubes to form large myotubes. Although the roles of myogenic regulatory factors (MRFs), including Myf5, Myod, Myogenin and Mrf4, in myogenic differentiation are unquestionable [3-5], a number of factors, such as secreted proteins, membrane proteins and transcriptional regulators, are also involved in myogenesis [2].

Microphthalmia-associated transcription factor (Mitf) is a member of the basic helix-loop-helix leucine zipper (bHLH-LZ) family of transcription factors [6-8]. Expression levels of Mitf, evaluated by Western blotting and Northern blotting, vary among tissues; it is highly expressed in melanocytes, mast cells, osteoclasts, and the heart [9-11]. Thus, the roles of Mitf have been mainly examined in these cells [11-14], and Mitf activities in other tissues are largely unknown. Of the *Mitf* variants that are not the result of genetic mutation, nine *Mitf* isoforms have been identified in mice that differ in their transcriptional initiation site: *Mitf-A*, *-B*, *-C*, *-D*, *-E*, *-H*, *-J*, *-M* and *-mc*. The *Mitf* variants contain an isoform-specific first exon, while exons 2 to 9 of all *Mitf* isoforms examined to date are identical. *Mitf* isoforms are expressed in a cell type-specific manner, and their transcriptional activities are slightly but significantly different depending on the target gene [15-19]. In addition, two types of *Mitf* mRNAs with or without an 18-base insert (exon 6a) are generated by alternative use of the two acceptor sites located at the 5’ end of exon 6 in *Mitf-A*, *-H*, *-J*, *-M* and *-mc* [6, 9, 20, 21]. In the

present study, we show the relatively higher expression of *Mitf-A* in the skeletal muscle, and present the potential role of Mitf in the progression of myogenesis.

Materials and methods

Animals and cell culture

Nine C57BL/6 mice aged 7-8 wk were used to examine the tissue distribution of Mitf. The experiment was approved by Azabu University Animal Experiment Committee. C2C12 myoblasts were obtained from the American Type Culture Collection (Rockville, MD). Cells were cultured in growth medium, i.e., Dulbecco's modified Eagle's medium (DMEM) with heat-inactivated 10% fetal bovine serum (FBS), 100 U/ml penicillin and 100 μg/ml streptomycin, at 37°C under a humidified 5% CO_2 atmosphere. To induce differentiation from myoblasts to myotubes, the medium was replaced at confluence (day 0) with differentiation medium consisting of DMEM with 2% horse serum supplementing the antibiotics. To isolate myotubes, cells on day 7 were trypsinized for a short time under a microscope until detachment of multinucleated cells (~2 min), followed by centrifugation to obtain a myotube-rich fraction.

RT-PCR, restriction fragment length polymorphism and quantitative RT-PCR

Total RNA isolation from tissues and cells, RT-PCR and restriction fragment length polymorphism (RFLP) were performed as described previously [21]. Quantitative RT-PCR (qRT-PCR) was carried out as described previously [22]. The used PCR primers in qRT-PCR are presented in Table 1. To compare tissue *Mitf* expression, the appropriate corrected gene was chosen using a mouse housekeeping gene primer set (TaKaRa, Otsu, Japan). The relative mRNA level was expressed as a ratio with *β-actin* to evaluate tissue distribution and *Gapdh* was used as a reference gene to examine regulatory expression in C2C12 cells.

Western blotting

To examine expression of Mitf in the skeletal muscle, thigh muscle and heart as a positive control were homogenized in RIPA buffer. After 30 min on ice, the debris was removed by centrifugation at 2,500 $\times$ *g* for 2 min at 4^{O}C. After centrifugation at 12,000 $\times$ *g* for 5 min at 4^{O}C, the supernatant was recovered and the protein concentration was measured by the bicinchoninic acid method [23]. Fifty μg of the protein was loaded on 10% SDS-polyacrylamide gel. Western blotting was performed as described previously [24, 25]. Expression of Mitf and myosin heavy chain (Myhc) was examined by use of mouse monoclonal antibodies against Mitf (X1405M; Exalpha Biologicals) and Myhc (MY-32; Sigma), respectively. There are two types of muscle fiber, i.e., fast-twitch and slow-twitch; fast-twitch muscle fibers express Myhc2a, Myhc2b and Myhc2x, whreas slow-twitch muscle fibers do Myhc1 [26]. According to the manufacturer's manual, this antibody for Myhc recognizes fast-type muscle fibers. After incubation of the membranes with ECL Advance reagent (GE Healthcare), the chemiluminescent signals were exposed to X-ray film. Subsequently, antibodies as well as the detection reagents were stripped and reprobed with anti-α-tubulin (ab11304; Abcam) or anti-β-actin antibody (AC-15; Abcam).

Immunohistochemistry

C2C12 cells were grown on glass chamber slides coated with type I collagen (Thermo Fisher Scientific) and were fixed with 3% paraformaldehyde in PBS for 30 min, followed by treatment with 1% Triton X-100 in PBS for 10 min. After washing with PBS, cells were incubated with 3% H_2O_2 to remove endogenous peroxidase. Subsequently, cells were treated with 1.5% normal goat serum in PBS for 20 min to block nonspecific reactions. Diluted mouse monoclonal antibody against Mitf (X1405M; Exalpha Biologicals) with 0.1% bovine serum albumin in PBS at 1 : 80 was

used to identify Mitf expression at the protein level. After incubation with the primary antibody for 2 h at room temperature, Mitf-positive cells were visualized using VECTASTAIN Elite ABC kit (Vector Laboratories) and 3,3’-diaminobenzidine (DAB; Dojindo) according to the manufacturer’s protocol.

siRNA transfection

To target the expression of common *Mitf, Mitf-A* or *Itga9* and *green fluorescent protein* (*GFP*) controls, oligonucleotides for the respective genes were synthesized by BONAC corporation (Kurume, Japan) as follows: 5'-GAAACUUGAUCGACCUCUACA-3' and 5'-UAGAGGUCGAUCAAGUUUCCA-3' for common *Mitf*, 5’-GGAGUCAUGCAGUCCGAAUTT -3’ and 5'- AUUCGGACUGCAUGACUCCTT -3' for *Mitf-A*, 5'-CCUUAGUGCUCUUCCGAAAGA-3' and 5'-UUUCGGAAGAGCACUAAGGUU-3' for *Itga9*, and 5’-GGUUACGUCCAGGAGCGCATT-3’ and 5'-UGCGCUCCUGGACGUAGCCTT-3' for *GFP*. The siRNA for *p21* was purchased (sc-29428; Santa Cruz Biotechnology). An equal amount of the oligonucleotide was mixed for each gene to prepare siRNA. Thirty picomoles of siRNA was transfected into C2C12 cells seeded at a density of 1.5×10^4 cells in 24-well plates every 48 h. siRNA was transfected using Lipofectamine RNAiMAX (Invitrogen) according to the manufacturer’s protocol. Antibiotics were not supplemented to the culture media in siRNA transfection experiments.

Morphological analysis

Cells were fixed with methanol for 2 min and subsequently stained with Giemsa staining for 20 min. Cells with more than 3 nuclei were judged as myotubes. Eight views per treatment in an experiment were analyzed. Experiments were repeated two or three times, and similar results were obtained.

BrdU incorporation

Proliferation of C2C12 cells was measured by a BrdU cell proliferation assay (Cell Proliferation ELISA, BrdU (colorimetric); Roche) according to the manufacturer's protocol.

Statistical analysis

Data are presented as the mean ± SE. Comparisons between groups were conducted using Student's *t*-test. Results were considered significant at $P < 0.05$.

Results

Expression of Mitf in tissues and during myogenesis

Tissue distribution of *Mitf* was quantified by qRT-PCR. First, the expressions of 12 genes, *Atp5f1*, *B2m*, *β-actin*, *Gapdh*, *Hprt1*, *Pgk1*, *Ppia*, *RpLp1*, *Rps18*, *Tbp*, *Tfrc*, and *Ywhaz*, were quantified for evaluation as appropriate corrected genes; quantitative PCR using cDNA prepared from equal amounts of total RNA revealed that *β-actin* expression was the most stable among the tested tissues, which were evaluated by "geNorm" (http://medgen.ugent.be/~jvdesomp/genorm/) (data not shown). Thus, the gene transcript level of *Mitf* was corrected for that of *β-actin* (Fig. 1A). Expression of *Mitf* was highest in the heart, as expected. Although Mitf is recognized as a tissue-restricted transcription factor [6-8], its expression was detected in a wide variety of tissues. In particular, expression in the skeletal muscle was relatively higher. Previous studies indicated *Mitf* expression in the skeletal muscle [9, 27], but the role of Mitf is not known. Thus, we characterized the expression and function of Mitf in the skeletal muscle and during myogenesis in detail. Examining Mitf isoforms differing in transcriptional initiation site in the skeletal muscle indicated that more than 99% of *Mitf*

was *Mitf-A*, and that *Mitf-H* and *-J* were also expressed significantly (Fig. 1B).

In a C2C12 myotube differentiation model, C2C12 myoblasts fuse to form multinucleated myotube cells upon serum starvation on day 0 [28]. To evaluate gene expression in C2C12 cells, we chose *Gapdh* instead of *β-actin* as a reference gene; qPCR using cDNA prepared from equal amount of total RNA indicated gradual decrease in *β-actin* expression with progression of myogenesis, whereas expression of *Gapdh* was relatively constant (Supplementary Fig. 1). Total *Mitf* expression level increased up to day 8 and then reached a plateau (Fig. 1C). Similar to the expression pattern in the skeletal muscle, *Mitf-A* was the main isoform (59-76% of total *Mitf*). In addition, *Mitf-J* but not *-H* was expressed. The expression pattern of *Mitf* isoform was constant during myogenesis; the ratio of *Mitf-A* to *Mitf-J* was 1.5 to 3.2 : 1. Expression of Mitf in the skeletal muscle and C2C12 cells was also verified at the protein level by Western blot analyses (Fig. 1D). In addition, consistent with the changes at the mRNA level, expression of Mitf protein was increased after differentiation stimulation (Fig. 1E). Furthermore, Mitf was exclusively localized in the nucleus of C2C12 cells (Fig. 1F). We also examined the ratio of gene transcripts of Mitf with exon 6a to that of Mitf without exon 6a by PCR-RFLP analyses; the ratios of *Mitf-A* and *Mitf-J* were relatively constant during myogenesis (Fig. 1G).

Disruption of Mitf expression inhibits myotube formation by blocking increased expression of p21 and Itga9 induction

To clarify the roles of Mitf in myogenesis, we evaluated effects of decreased expression of Mitf, which was achieved by transfection with siRNA for *Mitf* (Supplementary Fig. 2A, lanes 2 and 3, and B). Transfection of siRNA for common *Mitf* effectively decreased the emergence of multinucleated myotubes on day 6, as compared with *GFP* (Fig. 2A). Knockdown of *Mitf-A* also blocked the formation of thick myotubes (Fig. 2B,

Supplementary Fig. 2C). Morphological analyses on day 6 indicated that the number of multinucleated cells, which were defined as cells with more than 3 nuclei, was significantly decreased by transfection of siRNA for *Mitf* (Fig. 2C). We also evaluated the differentiated myotubes in detail; knockdown of *Mitf* increased the proportion of myotubes with 3 to 5 nuclei, but decreased that of myotubes with more than 6 nuclei (Fig. 2D). Similar results were also obtained in C2C12 cells transfected with siRNA for *Mitf-A* (Supplementary Fig. 3). Furthermore, *Mitf* knockdown decreased the expression of Myhc, a myotube-specific protein [3-5], in C2C12 cells on day 8 (Fig. 2E, lanes 1 and 2). These results suggest that Mitf is required not only for myoblast-myoblast fusion but also for maturation of nascent myotubes. We also examined effects of forced Mitf expression on myotube formation; the expression did not enhance myogenesis (data not shown).

Molecular bases of decreased myotube formation by *Mitf* knockdown were then explored. Myogenesis is regulated through modulation of the expression and activity of MRFs [29, 30]; however, gene transcript levels of *Myf5*, *Myod*, *Myogenin* and *Mrf4* were unchanged by *Mitf* knockdown, suggesting that impairment of myogenesis resulting from *Mitf* knockdown is not due to altered expression of MRFs (Fig. 3A-D).

Other than MRFs, several molecules related to cell attachment and fusion, such as *Adam12*, *Calpastatin*, *Caveolin3*, *Cdh15*, *Ctsb*, *Itga3*, *Itga4*, *Itga6*, *Itga9*, *Itgb1*, *Myof*, and *v-Cam1* are known to regulate myotube differentiation [2, 31-34]. In addition, the cDNA microarray database (http://www.ncbi.nlm.nih.gov/geo/) indicated that the expressions of *Ccna2*, *Itga5*, *p21*, *p57*, *Ptger4*, *Rb1*, and *Vcl* increased with differentiation. In view of Mitf as a transcription factor, we expected that Mitf is involved in myogenesis through transcriptional activation of these myogenesis-regulating genes. Thus, the effects of decrease in *Mitf* expression on the

expression level of these genes were explored. We found that gene transcript levels of *p21* and *Itga9* after differentiation stimulation were decreased by transfection of siRNA for common *Mitf*; expression of *p21* was increased in response to differentiation stimulation, and *Mitf* knockdown blocked the increased expression of *p21* (Fig. 3E). Significant expression of *Itga9* was detected after day 4, and the expression level was decreased by transfection of siRNA for *Mitf* (Fig. 3F). Decreased expression of *p21* and *Itga9* was also detected in *Mitf-A*-knockdown cells (Supplementary Fig. 4). Gene transcript levels of the other genes were unaffected by *Mitf* knockdown (Supplementary Fig. 5).

In a C2C12 myogenesis cell model, not all myoblasts not fuse into myotubes; co-existence of proliferating myoblasts and myotubes is detected after differentiation stimulation [35-37]. We separated the myotube-rich fraction by limited trypsinization to explore cells affected by *Mitf* knockdown. Although *Myhc2a* expression was not significantly different between the myotube fraction and the residual cell fraction in control cells (Fig. 4A), *Myhc2b* and *Myhc2x* were predominantly expressed in the myotube fraction as expected (Fig. 4B and C). Expression of *Myhc2x* in the myotube fraction was significantly lower in *Mitf*-knockdown cells than in control cells, whereas that of *Myhc2a* in the myotube fraction was higher in the *Mitf*-knockdown cells. The *Myhc2b* expression in the myotube fraction was comparable between in control cells and in *Mitf*-knockdown cells. Considering that *Myhc2x* was the major isoform of type 2 *Myhc* (> 93%) (Fig. 4D), total expression of *Myhc* constituting of fast-twitch myofibers was largely limited to the myotube fraction, and was decreased by *Mitf* knockdown; the latter was consistent with the results on Myhc expression at the protein level (Fig. 2E).

The extent of the decreased expression of *Mitf* resulting from knockdown of *Mitf* was comparable between the myotube fraction and the residual cell fraction, indicating

effective inhibition of *Mitf* expression in both myoblasts and myotubes (Fig. 5A). Expression of *p21* was significantly higher in the myotube fraction than in the residual cell fraction (Fig. 5B). Knockdown of *Mitf* equally decreased the expression of between the two fractions. Expression of *Itga9* was also significantly higher in the myotube fraction (Fig. 5C). Similar to the expression of *p21*, *Mitf* knockdown down-regulated the expression of *Itga9* in both fractions.

Cell cycle exit in response to differentiation stimulation is a prerequisite for myotube formation [2]; p21, a cyclin-dependent kinase inhibitor inducing cell cycle exit, plays a role in post-mitotic myogenesis, although it also maintains anti-apoptotic states in differentiated myocytes [1]. To link the decreased *Mitf*-induced inhibition of myotube formation and blockage of *p21* induction, effects of the decreased *Mitf* expression on BrdU uptake were next examined; BrdU uptake was significantly increased by transfection of siRNA for *Mitf* on day 4-6 (Fig. 5A). Knockdown of *p21*, however, did not affect BrdU uptake (Fig. 5B). Similar to *Mitf* knockdown, decreased expression of p21 inhibited emergence of maturated and thick myotubes (Fig. 5C). In addition, it significantly decreased the number of multinucleated cells (Fig. 5D), and increased and decreased the proportion of myotubes with 3 to 5 nuclei and those with more than 6 nuclei, respectively (Fig. 5E).

We next explored the effects of Itga9 knockdown on myotube formation. The morphology of cells transfected with siRNA for *Itga9* indicated that, compared to control cells, thinner myotubes were evident by *Itga9* knockdown, suggesting that Itga9 is required for myotube maturation (Fig. 6A), which was verified by morphometry. The multinucleated cell number itself was not affected by knockdown of *Itga9* (Fig. 6B), but the proportion of the number of myotubes with 3-5 nuclei in a cell to that of total myotubes was significantly increased, and that with more than 6 nuclei was decreased

(Fig. 6C). Consistent with the results, knockdown of *Itga9* gene resulted in the decreased expression of Myhc (Fig. 2E, lanes 1 and 3).

Discussion

Here, we demonstrate that 1) A isoform of *Mitf* mRNA is abundant in the skeletal muscle, 2) *Mitf-A* expression increased with progression of myogenesis, 3) knockdown of *Mitf* mRNA disrupts myotube formation through inhibition of myoblast-myoblast fusion and subsequent myoblast-myotube fusion, but does not affect the expression of MRFs, and 4) expression of *p21*, a cyclin-dependent kinase inhibitor, and *Itga9* is regulated by Mitf in a stage-dependent manner for appropriate myogenesis. The present results indicate a novel role of a tissue-restricted transcription factor Mitf in the regulation of myogenesis, which is probably mediated by an MRF-independent pathway.

Mitf regulates myogenesis in multiple steps. Expression of *p21* and *Itga9* was modulated by decreased expression of *Mitf*; down-regulation of *p21* expression resulting from knockdown of *Mitf* mRNA was limited to post-differentiation, and significant *Itga9* expression was detected just after differentiation stimulation. Considering that significant expression of *Mitf* was detected prior to differentiation stimulation, the gene expression of *p21* and *Itga9* could not be regulated by Mitf alone, but in concert with Mitf and as yet unidentified factor(s). Transfection of siRNA for *Mitf* resulted in down-regulated expression of *Mitf* both in myoblasts and myotubes. Thus, the precise mechanism of how Mitf regulates not only *p21* in myoblasts and myotubes but also *Itga9* expression in myotubes remains unclear. Since Mitf binds to the E-box (CAnnTG) located in the 5'-untranslated region and activates transcription [6-8], Mitf may directly regulate transcription of *p21* and *Itga9*. Alternatively, it is possible that a factor

regulated by Mitf in myoblasts acts as a regulator to induce *p21* or *Itga9* in myotubes.

A target gene of Mitf was *Itga9*. Among members of the integrin family, Itga3, 4, 6 and 9 have been suggested to regulate myogenesis [2, 31, 33, 34]. Transcription of *Itga4* was activated through Mitf binding to the E-box located in the 5'-untranslated region in mast cells [38]. In the present study, however, *Itga4* mRNA was not decreased but rather increased by transfection of siRNA for *Mitf* in C2C12 cells (Supplementary Fig. 2H), suggesting that transcription by Mitf is regulated in a cell context-dependent manner. In addition, *Mitf* knockdown did not affect the expression level of *Itga3* and *6* (Supplementary Fig. 2G and J). In a study using a human mononucleated myogenic precursor cell culture system, addition of anti-INTEGRIN $\alpha 9\beta 1$ antibody to the culture medium decreased the proportion of nuclei included in large myotubes ($\geq$5 nuclei), whereas the proportion of nuclei incorporated in small myotubes (2-4 nuclei) was unchanged [33]. In the present study using a murine myogenesis model, transfection with siRNA for *Itga9* decreased the proportion of large myotubes ($\geq$6 nuclei) and increased that of small myotubes (3-5 nuclei), but did not affect the number of multinucleated cells. Taking these results together, Itga9 is suggested to promote the growth of preformed myotubes rather than the formation of nascent myotubes during myogenesis.

Effects of knockdown of *Mitf* mRNA partly overlapped but were distinct from those of *Itga9* knockdown; the number of multinucleated cells was decreased by *Mitf* knockdown. This suggests that Mitf is involved in both myoblast-myoblast fusion and subsequent maturation of nascent myotubes. It is possible that Mitf regulates myoblast-myoblast fusion through the increase in p21 expression; regulatory expression of *p21* by Mitf has also been shown in melanocytes [39]. Cell cycle inhibition and apoptosis of myoblasts precede to myoblast-myoblast fusion, and both processes are

necessary for the cell fusion [1]. p21 is principally involved as a molecule to establish post-mitotic and apoptosis-resistant states [1]; BrdU uptake was not detected in p21-positive myoblasts [40], and forced expression of p21 but not inactive p21 inhibited apoptosis of C2C12 myoblasts [41]. In fact, *p21* knockdown decreased the myotube number and increased proportion of small myotubes, suggesting that p21 expression is required for efficient myoblast-myoblast fusion.

Knockdown of *p21* did not increase BrdU uptake on day 4 and 6; it may be offset effects of the cell growth inhibition and the anti-apoptotic activity. In view of significant inhibition of BrdU uptake in *Mitf*-knockdown cells on day 4 and 6, Mitf regulates expression and activity of additional molecule(s) unidentified in this study.

Bharti et al. [19] revealed that *Mitf-A* and *-J* are expressed throughout eye development in both retina and pigment epithelium, whereas expression of *Mitf-D* and *-M* was limited to pigment epithelium. In addition, *Mitf-H* was preferentially found in pigment epithelium with temporal expression profile. Unlike the eye development, the proportion of expressed *Mitf* isoforms, i.e., *Mitf-A* and *Mitf-J* was almost constant during myogenesis of C2C12 cells, although total *Mitf* expression was increased with progression of myogenesis (Fig. 1C). Thus, expression of *Mitf* isoforms is tissue-specific and stage-dependent. In view of different activity as transcription factors between the isoforms [15-18], regulation on the use of alternative promoter must be clarified in future studies.

Mitf encoded by the mutant *mi* allele deletes one of four consecutive arginines in the basic domain, and acts as a dominant-negative mutant [9, 27, 42]. The *mi/mi* mutant mice exhibited the pleiotropic effects of microphthalmia, depletion of pigment in both hair and eyes, and osteopetrosis resulting from defects of osteoclastogenesis [9, 14]. In

addition to these phenotype alterations, Katayama et al. [43] recently showed that masseter muscle development was disrupted in *mi/mi* mutant mice; they speculated that the disorder is a secondary event related to abnormal tooth formation related to osteoclast dysfunction; however, in view of the present results showing direct inhibition of myogenesis by decreased expression of *Mitf*, muscle development itself may be disturbed in *mi/mi* mice.

The present study indicates significant expression of *Mitf* in the skeletal muscle from re-evaluation of tissue distribution of *Mitf* by sensitive qRT-PCR analyses. Evaluation of Mitf activity clarifies its role as a positive regulator during myogenesis. Because Mitf is expressed also in other tissues with a variation of expression level, future studies should be directed to elucidate the role of Mitf in as yet uncharacterized tissues.

Acknowledgements

This work was supported by Kakenhi from The Japan Society for the Promotion of Science, and a research project grant awarded by the Azabu University.

References

[1] K. Walsh, H. Perlman, Cell cycle exit upon myogenic differentiation, Curr. Opin. Genet. Dev. 7 (1997) 597-602.

[2] V. Horsley, G.K. Pavlath, Forming a multinucleated cell: molecules that regulate myoblast fusion, Cells Tissues Organs 176 (2004) 67-78.

[3] D.C. Ludolph, S.F. Konieczny, Transcription factor families: muscling in on the myogenic program, FASEB J. 9 (1995) 1595-1604.

[4] R.L. Perry, M.A. Rudnicki, Molecular mechanisms regulating myogenic determination and differentiation, Front Biosci. 5 (2000) D750-D767.

[5] F. Lluís, E. Perdiguero, A.R. Nebreda, P. Muñoz-Cánoves, Regulation of skeletal muscle gene expression by p38 MAP kinases, Trends Cell Biol. 16 (2006) 36-44.

[6] K. Yasumoto, S. Amae, T. Udono, N. Fuse, K. Takeda, S. Shibahara, A big gene linked to small eyes encodes multiple Mitf isoforms: many promoters make light work, Pigment Cell Res. 11 (1998) 329-336.

[7] Y. Kitamura, E. Morii, T. Jippo, A. Ito, mi-transcription factor as a regulator of mast cell differentiation, Int. J. Hematol. 71 (2000) 197-202.

[8] H.R. Widlund, D.E. Fisher, Microphthalamia-associated transcription factor: a critical regulator of pigment cell development and survival, Oncogene 22 (2003) 3035-3041.

[9] E. Steingrímsson, K.J. Moore, M.L. Lamoreux, A.R. Ferré-D'Amaré, S.K. Burley, D.C. Zimring, L.C. Skow, C.A. Hodgkinson, H. Arnheiter, N.G. Copeland, N.A. Jenkins, Molecular basis of mouse microphthalmia (mi) mutations helps explain their developmental and phenotypic consequences, Nat. Genet. 8 (1994) 256-263.

[10] K.N. Weilbaecher, C.L. Hershey, C.M. Takemoto, M.A. Horstmann, T.J. Hemesath, A.H. Tashjian, D.E. Fisher, Age-resolving osteopetrosis: a rat model implicating microphthalmia and the related transcription factor TFE3, J. Exp. Med. 187 (1998) 775-785.

[11] S. Tshori, D. Gilon, R. Beeri, H. Nechushtan, D. Kaluzhny, E. Pikarsky, E. Razin, Transcription factor MITF regulates cardiac growth and hypertrophy, J. Clin. Invest. 116 (2006) 2673-2681.

[12] Y. Kitamura, E. Morii, T. Jippo, A. Ito, Regulation of mast cell phenotype by MITF, Int. Arch. Allergy Immunol. 127 (2002) 106-109.

[13] C.L. Hershey, D.E. Fisher, Mitf and Tfe3: members of a b-HLH-ZIP transcription factor family essential for osteoclast development and function, Bone 34 (2004) 689-696.

[14] E. Steingrímsson, N.G. Copeland, N.A. Jenkins, Melanocytes and the microphthalmia transcription factor network, Annu. Rev. Genet. 38 (2004) 365-411.

[15] S. Amae, N. Fuse, K. Yasumoto, S. Sato, I. Yajima, H. Yamamoto, T. Udono, Y.K. Durlu, M. Tamai, K. Takahashi, S. Shibahara, Identification of a novel isoform of microphthalmia-associated transcription factor that is enriched in retinal pigment epithelium, Biochem. Biophys. Res. Commun. 247 (1998) 710-715.

[16] C.M. Takemoto, Y.J. Yoon, D.E. Fisher, The identification and functional characterization of a novel mast cell isoform of the microphthalmia-associated transcription factor, J. Biol. Chem. 277 (2002) 30244-30252.

[17] M. Murakami, T. Ikeda, K. Ogawa, M. Funaba, Transcriptional activation of mouse mast cell protease-9 by microphthalmia-associated transcription factor, Biochem. Biophys. Res. Commun. 311 (2003) 4-10.

[18] M. Funaba, T. Ikeda, M. Murakami, K. Ogawa, M. Abe, Up-regulation of mouse mast cell protease-6 gene by transforming growth factor-β and activin in mast cell progenitors, Cell. Signal. 17 (2005) 121-128.

[19] K. Bharti, W. Liu, T. Csermely, S. Bertuzzi, H. Arnheiter, Alternative promoter use in eye development: the complex role and regulation of the transcription factor MITF, Development 135(2008) 1169-1178.

[20] J.H. Hallsson, J. Favor, C. Hodgkinson, T. Glaser, M.L. Lamoreux, R. Magnúsdóttir, G.J. Gunnarsson, H.O. Sweet, N.G. Copeland, N.A. Jenkins, E. Steingrímsson, Genomic, transcriptional and mutational analysis of the mouse microphthalmia locus, Genetics 155 (2000) 291-300.

[21] M. Murakami, Y. Iwata, M. Funaba, Expression and transcriptional activity of alternative splice variants of Mitf exon 6, Mol. Cell. Biochem. 303 (2007) 251-257.

[22] M. Murakami, H. Kawachi, K. Ogawa, Y. Nishino, M. Funaba, Receptor expression modulates the specificity of transforming growth factor-β signaling pathways, Genes Cells 14 (2009) 469-482.

[23] P.K. Smith, R.I. Krohn, G.T. Hermanson, A.K. Mallia, F.H. Gartner, M.D. Provenzano, E.K. Fujimoto, N.M. Goeke, B.J. Olson, D.C. Klenk, Measurement of protein using bicinchoninic acid, Anal. Biochem. 150(1985) 76-85.

[24] M. Funaba, M. Murakami, A sensitive detection of phospho-Smad1/5/8 and Smad2 in Western blot analyses, J. Biochem. Biophys. Methods 70 (2008) 816-819.

[25] M. Suenaga, T. Matsui, M. Funaba, BMP Inhibition with dorsomorphin limits adipogenic potential of preadipocytes, J. Vet. Med. Sci.72 (2010) 373-377.

[26] S. Schiaffino, C. Reggiani, Molecular diversity of myofibrillar proteins: gene regulation and functional significance, Physiol. Rev. 76 (1996) 371-423.

[27] C.A. Hodgkinson, K.J. Moore, A. Nakayama, E. Steingrímsson, N.G. Copeland, N.A. Jenkins, H. Arnheiter, Mutations at the mouse microphthalmia locus are associated with defects in a gene encoding a novel basic-helix-loop-helix-zipper protein, Cell 74 (1993) 395-404.

[28] D. Yaffe, O. Saxel, Serial passaging and differentiation of myogenic cells isolated from dystrophic mouse muscle, Nature 270 (1977) 725-727.

[29] F. Viñals, F. Ventura, Myogenin protein stability is decreased by BMP-2 through a mechanism implicating Id1, J. Biol. Chem. 279 (2004) 45766-45772.

[30] Y. Furutani, T. Umemoto, M. Murakami, T. Matsui, M. Funaba, Role of endogenous TGF-β family in myogenic differentiation of C2C12 cells, J. Cell. Biochem. 112 (2011) 614-624.

[31] S.K. Sastry, M. Lakonishok, D.A. Thomas, J. Muschler, A.F. Horwitz, Integrin α subunit ratios, cytoplasmic domains, and growth factor synergy regulate muscle proliferation and differentiation, J. Cell Biol. 133 (1996) 169-184.

[32] K.R. Doherty, A. Cave, D.B. Davis, A.J. Delmonte, A. Posey, J.U. Earley, M. Hadhazy, E.M. McNally, Normal myoblast fusion requires myoferlin, Development 132 (2005) 5565-5575.

[33] P. Lafuste, C. Sonnet, B. Chazaud, P.A. Dreyfus, R.K. Gherardi, U.M. Wewer, F.J. Authier, ADAM12 and α9β1 integrin are instrumental in human myogenic cell differentiation, Mol. Biol. Cell 16 (2005) 861-870.

[34] E. Brzóska, V. Bello, T. Darribère, J. Moraczewski, Integrin α3 subunit participates in myoblast adhesion and fusion in vitro, Differentiation 74 (2006) 105-118.

[35] M. Kitzmann, G. Carnac, M. Vandromme, M. Primig, N.J. Lamb, A. Fernandez, The muscle regulatory factors MyoD and Myf-5 undergo distinct cell cycle-specific expression in muscle cells, J. Cell Biol. 142 (1998) 1447-1459.

[36] N. Yoshida, S. Yoshida, K. Koishi, K. Masuda, Y. Nabeshima, Cell heterogeneity upon myogenic differentiation: down-regulation of MyoD and Myf-5 generates 'reserve cells', J. Cell Sci. 111 (1998) 769-779.

[37] M. Menconi, P. Gonnella, V. Petkova, S. Lecker, P.O. Hasselgren, Dexamethasone and corticosterone induce similar, but not identical, muscle wasting responses in cultured L6 and C2C12 myotubes, J. Cell. Biochem. 105 (2008) 353-364.

[38] D.K. Kim, E. Morii, H. Ogihara, K. Hashimoto, K. Oritani, Y.M. Lee, T. Jippo, S. Adachi, Y. Kanakura, Y. Kitamura, Impaired expression of integrin α-4 subunit in cultured mast cells derived from mutant mice of mi/mi genotype, Blood 92 (1998) 1973-1980.

[39] S. Carreira, J. Goodall, I. Aksan, S.A. La Rocca, M.D. Galibert, L. Denat, L. Larue, C.R. Goding, Mitf cooperates with Rb1 and activates p21Cip1 expression to regulate cell cycle progression, Nature 433 (2005) 764-769.

[40] V. Andrés, K. Walsh, Myogenin expression, cell cycle withdrawal, and phenotypic differentiation are temporally separable events that precede cell fusion upon myogenesis, J. Cell Biol. 132 (1996) 657-666.

[41] J. Wang, K. Walsh, Resistance to apoptosis conferred by Cdk inhibitors during myocyte differentiation, Science 273 (1996) 359-361.

[42] T.J. Hemesath, E. Steingrímsson, G. McGill, M.J. Hansen, J. Vaught, C.A. Hodgkinson, H. Arnheiter, N.G. Copeland, N.A. Jenkins, D.E. Fisher, microphthalmia, a critical factor in melanocyte development, defines a discrete transcription factor family, Genes Dev. 8 (1994) 2770-2780.

[43] R. Katayama, A. Yamane, T. Fukui, Changes in the expression of myosins during postnatal development of masseter muscle in the microphthalmic mouse, Open Dent. J. 4 (2010) 1-7.

Figure legends

Fig. 1. Mitf expression is highly expressed in the skeletal muscle and increases with progression of myogenesis in C2C12 cells

(A) *Mitf* expression in various tissues was measured by qRT-PCR. *Mitf* expression was expressed as a ratio to *β-actin* expression. Data are shown as the mean ± SE. (B) Expression of *Mitf* isoform differing with transcriptional initiation site in the skeletal muscle was identified by qRT-PCR using isoform-specific 5'-primer and 3'-primer spanning the common *Mitf*. The percentage of the expression of each *Mitf* isoform to that of total *Mitf* was calculated. Data are shown as the mean ± SE. (C) C2C12 myoblasts were cultured to confluence (day 0) in growth medium, followed by culture in differentiation medium. Time-course changes in expression of *Mitf* isoform differing with transcriptional initiation site during myogenesis were examined in C2C12 cells. *Mitf* expression was expressed as a ratio to *Gapdh* expression. Data are shown as the mean ± SE (n = 2). (D) Expression of Mitf in the skeletal muscle. Protein extracted from heart, thigh muscle and C2C12 cells was subjected to Western blot analyses to examine Mitf expression at the protein level. A representative result of Western blot is shown. In the heart, Mitf-H as well as Mitf-A is mainly expressed shown in (B). Note that calculated molecular weight of Mitf-H and Mitf-A is 56.8 k and 58.6 k, respectively. (E) Time-course changes in expression of Mitf protein were examined during myogenesis of C2C12 cells. A representative result of Western blot is shown. (F) Immunolocalization of Mitf in C2C12 cells. C2C12 myoblasts were fixed and reacted with (*right*) or without (*left*) mouse monoclonal anti-Mitf antibody. Subsequently, cells were reacted with anti-mouse IgG antibody, and the antibody was visualized. A representative cell staining is shown. (G) The ratio of exon 6a-containing *Mitf* isoforms (exon 6a + 6b) to non-exon 6a-containing isoforms (exon 6b) was evaluated in C2C12 cells. PCR products of *Mitf -A* and *-J* were digested by *Hinf* I, and DNA fragments with or without exon 6a were separated by PAGE. A photograph of a representative gel

stained with ethidium bromide is shown.

Fig. 2. Mitf expression is required for efficient myotube formation

C2C12 cells were transfected with siRNA for *GFP* as a control, common *Mitf* or *Mitf-A* every 2 days after day -2. (A) Effect of *Mitf* knockdown on myogenesis was evaluated. Representative phase-contrast images on day 0, 2, 4, and 6 are presented. (B) Role of Mitf-A was examined. Representative cells stained by Giemsa solution on day 6 are presented. (C and D) Myotube formation was evaluated in *Mitf*-knockdown C2C12 cells. Cells were transfected with siRNA for *GFP* as a control or *Mitf*, and morphology was evaluated on day 6. After staining with Giemsa solution, cell number and the number of nuclei were calculated. (C) Ratio of multinucleated cell number to total cell number was calculated, and the ratio of cells transfected with siRNA for *GFP* was set to 1. (D) Number of cells with 3 to 5, 6 to 10 or >11 nuclei were counted, and percentage to total multinucleated cells is shown. Data are shown as the mean ± SE (n = 6). * and **: $P < 0.05$ and $P < 0.01$, respectively, as compared to control. (E) Expression of Myhc in response to transfection of siRNA for *GFP* as a control, *Mitf* or *Itga9* in C2C12 cells on day 8 was examined by Western blot analyses. Subsequently, the membranes were reprobed with anti-β-actin antibody.

Fig. 3. p21 and Itga9 are targets of Mitf for progression of myogenesis

C2C12 cells were transfected with siRNA for *GFP* as a control or common *Mitf* every 2 days after day -2. Gene expression of *Myf5* (A), *Myod* (B), *Myogenin* (C), *Mrf4* (D), *p21* (E) and *Itga9* (F) was quantified by qRT-PCR. The expression was normalized to *Gapdh* expression. The expression in cells on day -2 was set to 1 for *Myf5*, *Myod*, *Myogenin*, *Mrf4* and *p21*, and that in cells transfected with siRNA for *GFP* on day 4 was set to 1 for *Itga9*. Data are shown as the mean ± SE (n = 2).

Fig. 4. Knockdown of Mitf in myoblasts and myotubes down-regulates expression of Myhc2x

C2C12 cells were transfected with siRNA for *GFP* as a control or common *Mitf* every 2 days after day -2. On day 7, multinucleated myotubes were separated from the residual cells by limited trypsinization. Expression of *Myhc2a* (A), *Myhc2b* (B) and *Myhc2x* (C) was quantified by qRT-PCR, and normalized to *Gapdh* expression. The expression in residual cells after limited trypsinization in the control group was set to 1. (D) The percentage of the expression of each *Myhc* isoform to that of total type II *Myhc* was calculated. Data are shown as the mean ± SE (n = 3). a, b, c, d: Means that do not have a common letter on the bar differ significantly ($P < 0.05$).

Fig. 5. Knockdown of Mitf in myoblasts and myotubes down-regulates expression of p21 and Itga9

C2C12 cells were transfected with siRNA for *GFP* as a control or common *Mitf* every 2 days after day -2. On day 7, multinucleated myotubes were separated from the residual cells by limited trypsinization. Expression of *Mitf* (A), *p21* (B), and *Itga9* (C) was quantified by qRT-PCR, and normalized to *Gapdh* expression. The expression in residual cells after limited trypsinization in the control group was set to 1. Data are shown as the mean ± SE (n = 3). a, b, c, d: Means that do not have a common letter on the bar differ significantly ($P < 0.05$).

Fig. 6. p21 is involved in Mitf-mediated myogenesis

(A and B) Role of Mitf and p21 in BrdU uptake in C2C12 cells was evaluated. (A) Cells were transfected with siRNA for *GFP* as a control or common *Mitf* every 2 days after day -2, and BrdU uptake was examined on day -1, 0, 4 and 6. BrdU uptake in control cells on day -1 was set to 100. (B) Cells were transfected with siRNA for *GFP* or *p21* every 2 days after day 2, and BrdU uptake was examined on day 4 and 6. Data are

shown as the mean ± SE (n = 3-4). **: *P* <0.01, as compared to control. (C-E) Role of p21 in myogenesis was evaluated. Cells were transfected with siRNA for *GFP* or *p21* every 2 days after day 2. (C) Representative cells stained by Giemsa solution on day 6 are shown. (D and E) Myotube formation was evaluated in *p21*-knockdown C2C12 cells. After staining cells with Giemsa solution on day 6, cell number and the number of nuclei were calculated. (D) Ratio of multinucleated cell number to total cell number was calculated, and the ratio of cells transfected with siRNA for *GFP* was set to 1. (E) Number of cells with 3 to 5, 6 to 10 or >11 nuclei was counted, and percentage to total multinucleated cells is shown. Data are shown as the mean ± SE (n = 4). * and **: *P* < 0.05 and *P* <0.01, respectively, as compared to control.

Fig. 7. Itga9 are involved in Mitf-mediated myogenesis

(A-C) Role of Itga9 in myogenesis was evaluated. Cells were transfected with siRNA for *GFP* or *Itga9* every 2 days after day -2. (A) Representative cells stained by Giemsa solution on day 6 are shown. (B and C) Myotube formation was evaluated in *Itga9*-knockdown C2C12 cells. After staining cells with Giemsa solution on day 6, cell number and the number of nuclei were calculated. (B) Ratio of multinucleated cell number to total cell number was calculated, and the ratio of cells transfected with siRNA for *GFP* was set to 1. (C) Number of cells with 3 to 5, 6 to 10 or >11 nuclei was counted, and percentage to total multinucleated cells is shown. Data are shown as the mean ± SE (n = 4). **: *P* <0.01, as compared to control.

Supplementary Fig. 1 Time-course changes in expression of Gapdh and β-actin during myogenesis of C2C12 cells

C2C12 myoblasts were cultured to reach confluence (day 0) in growth medium, followed by culture in differentiation medium. Expression of *Gapdh* and *β-actin* using

cDNA prepared from 5 ng of total RNA was quantified by qRT-PCR, and normalized to *Hprt1* expression. The expression on day 0 was set to 1. Data are shown as the mean ± SE (n = 2).

Supplementary Fig. 2 Effects of Mitf knockdown on Mitf expression in C2C12 cells

(A) C2C12 cells were transfected with siRNA for *GFP* as a control (c, lane 2) or common *Mitf* (M, lane 3) for 2 days. Western blot analyses were performed to examine Mitf expression. As a positive control, lysates of B16 melanoma cells were used (lane 1). B16 cells express mainly Mitf-M, whereas C2C12 cells predominantly express Mitf-A as shown in Fig. 1C. Note that calculated molecular weight of Mitf-M (46.8 k) is smaller than that of Mitf-A (58.6 k). (B and C) C2C12 cells were transfected with siRNA for *GFP* as a control, common *Mitf* or *Mitf-A* every 2 days after day -2. Gene expression of common *Mitf* (B) and *Mitf-A* (C) was quantified by qRT-PCR. The expression was normalized to *Gapdh* expression. The expression in cells on day -2 was set to 1. Data are shown as the mean ± SE (n = 2).

Supplementary Fig. 3 Impaired myotube formation in C2C12 cells transfected with siRNA for Mitf-A

C2C12 cells were transfected with siRNA for *GFP* as a control or *Mitf-A* every 2 days after day -2. (A and B) Myotube formation was evaluated in *Mitf-A*-knockdown C2C12 cells. Cells were transfected with siRNA for *GFP* as a control or *Mitf-A*, and morphology was evaluated on day 6. After staining with Giemsa solution, cell number and the number of nuclei were calculated. (A) Ratio of multinucleated cell number to total cell number was calculated, and the ratio of cells transfected with siRNA for *GFP* was set to 1. (B) Number of cells with 3 to 5, 6 to 10 or >11 nuclei were counted, and percentage to total multinucleated cells is shown. Data are shown as the mean ± SE (n =

6). * and **: $P < 0.05$ and $P < 0.01$, respectively, as compared to control.

Supplementary Fig. 4 Decreased expression of p21 and Itga9 in C2C12 cells transfected with siRNA for Mitf-A

C2C12 cells were transfected with siRNA for *GFP* as a control or *Mitf-A* every 2 days after day -2. Gene expression of *p21* (A) and *Itga9* (B) was quantified by qRT-PCR. The expression was normalized to *Gapdh* expression. The expression in cells transfected with siRNA for *GFP* on day -2 was set to 1. Data are shown as the mean ± SE (n = 2).

Supplementary Fig. 5 Effects of Mitf knockdown on gene expression in C2C12 cells

C2C12 cells were transfected with siRNA for *GFP* as a control or common *Mitf* every 2 days after day -2. Gene expression of *Adam12* (A), *Calpastatin* (B), *Caveolin3* (C), *Ccna2* (D), *Cdh15* (E), *Ctsb* (F), *Itga3* (G), *Itga4* (H), *Itga5* (I), *Itga6* (J), *Itgb1* (K), *Myof* (L), *p57* (M), *Ptger4* (N), *Rb1* (O), *v-Cam1* (P), and *Vcl* (Q) was quantified by qRT-PCR. The expression was normalized to *Gapdh* expression. The expression in cells on day -2 was set to 1. Data are shown as the mean ± SE (n = 2).

Figure 1A-E (Ooishi)

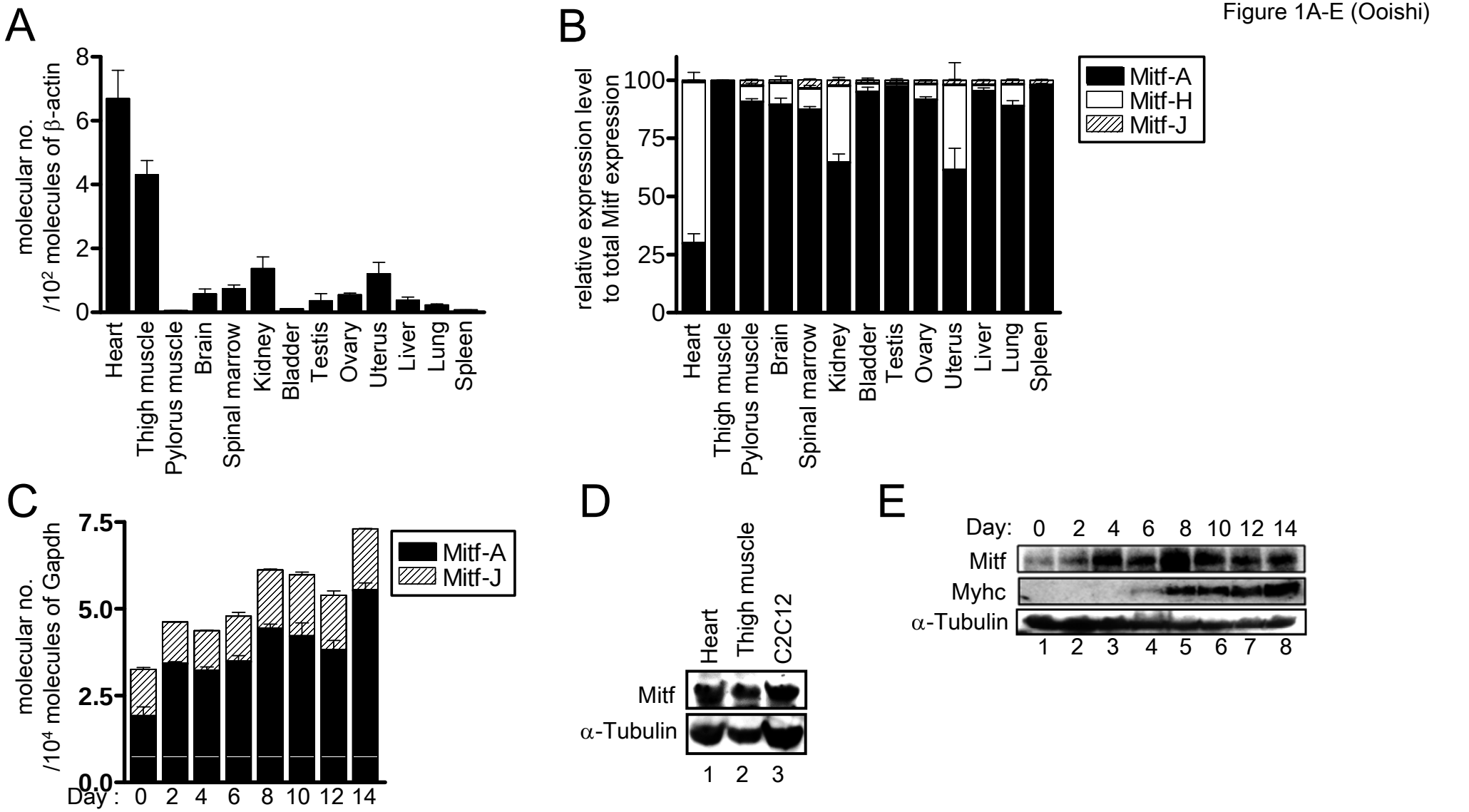

F

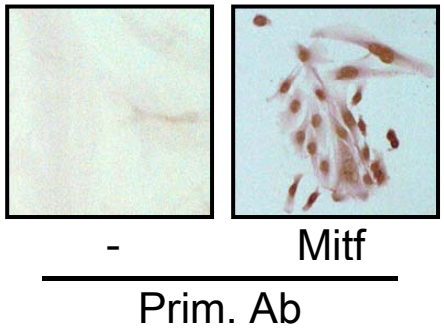
-
Mitf
Prim. Ab

G

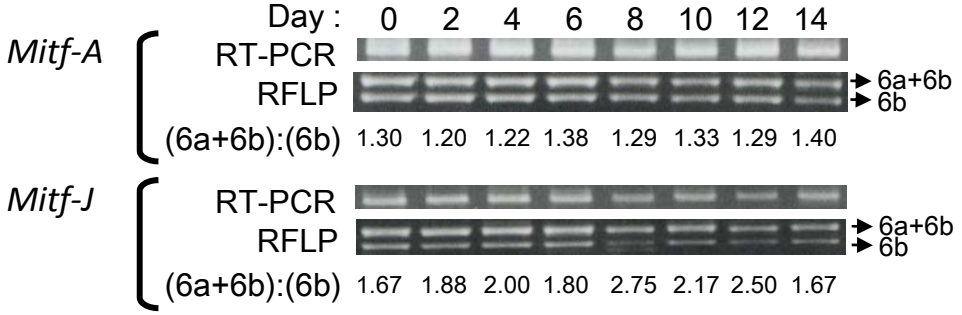
Day : 0 2 4 6 8 10 12 14
Mitf-A
RT-PCR
RFLP
6a+6b
6b
(6a+6b):(6b) 1.30 1.20 1.22 1.38 1.29 1.33 1.29 1.40
Mitf-J
RT-PCR
RFLP
6a+6b
6b
(6a+6b):(6b) 1.67 1.88 2.00 1.80 2.75 2.17 2.50 1.67

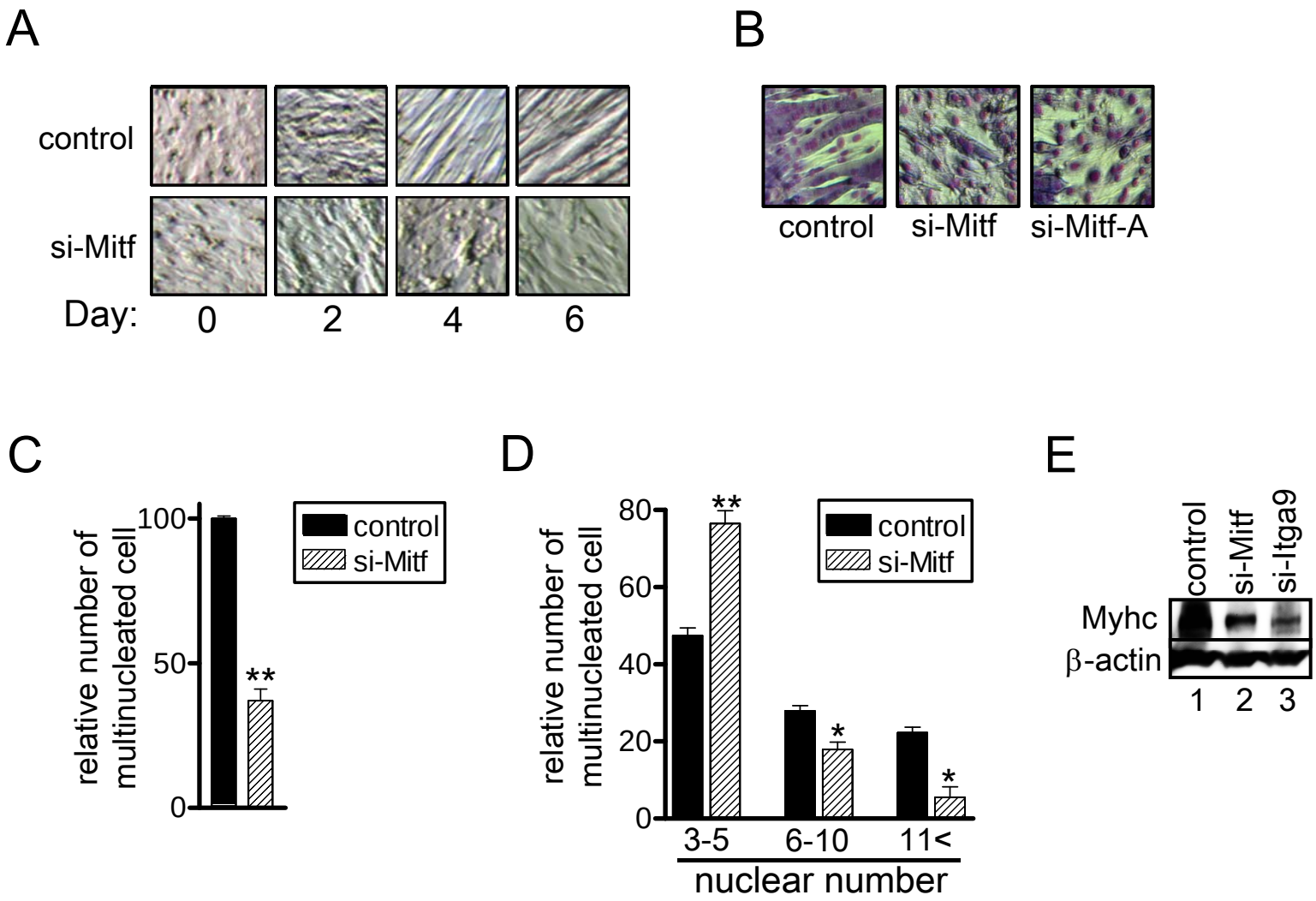
A
control
si-Mitf
Day:
0
2
4
6
B
control
si-Mitf
si-Mitf-A
C
relative number of multinucleated cell
100
50
0
control
si-Mitf
**
D
relative number of multinucleated cell
80
60
40
20
0
control
si-Mitf
**
*
*
3-5
6-10
11<
nuclear number
E
control
si-Mitf
si-Itga9
Myhc
β-actin
1
2
3

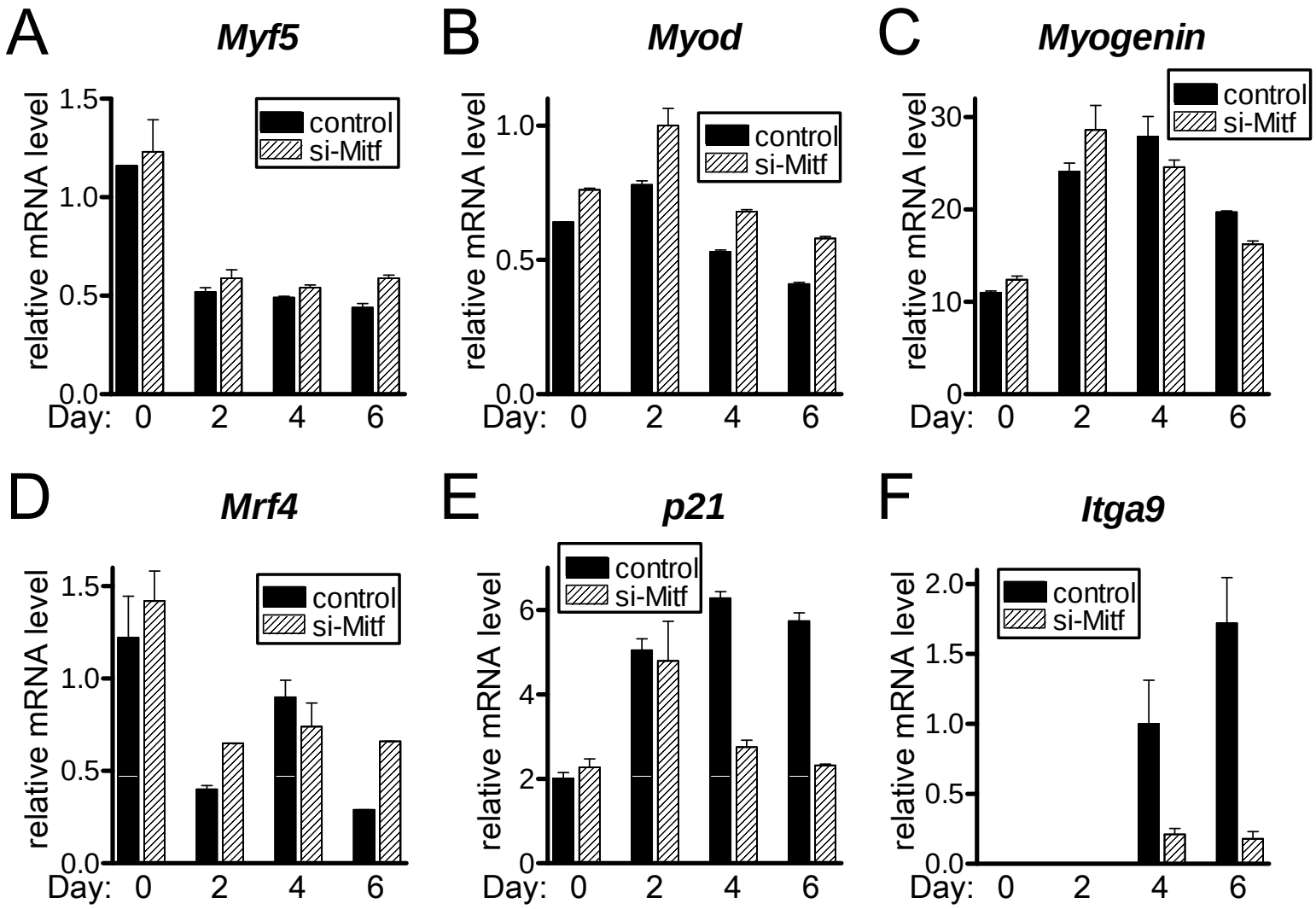
A
Myf5
B
Myod
C
Myogenin
D
Mrf4
E
p21
F
Itga9
relative mRNA level
control
si-Mitf
Day: 0 2 4 6

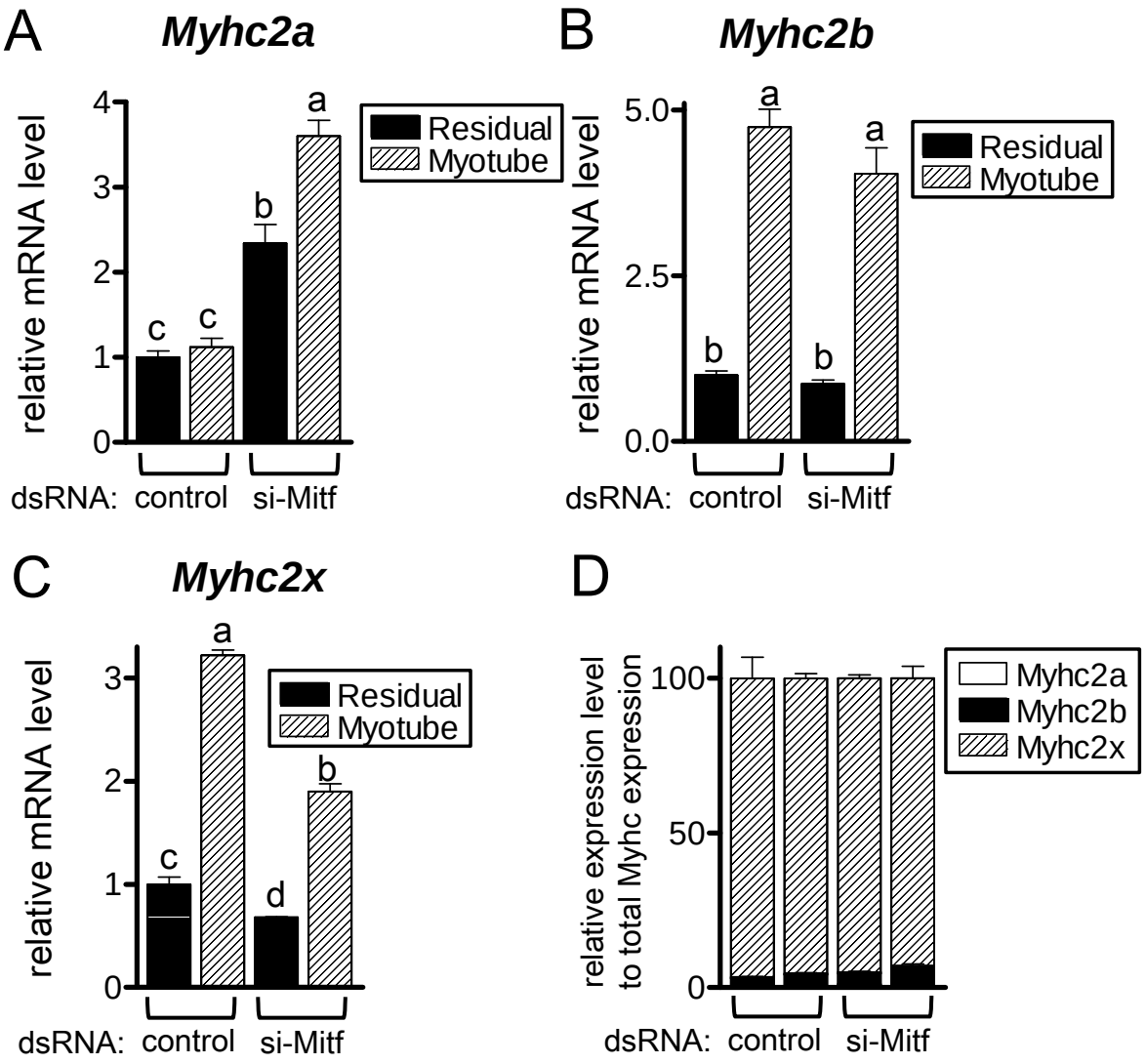
A
Myhc2a
relative mRNA level
4
3
2
1
0
c
c
b
a
Residual
Myotube
dsRNA: control si-Mitf
B
Myhc2b
relative mRNA level
5.0
2.5
0.0
b
b
a
a
Residual
Myotube
dsRNA: control si-Mitf
C
Myhc2x
relative mRNA level
3
2
1
0
c
d
b
a
Residual
Myotube
dsRNA: control si-Mitf
D
relative expression level to total Myhc expression
100
50
0
Myhc2a
Myhc2b
Myhc2x
dsRNA: control si-Mitf

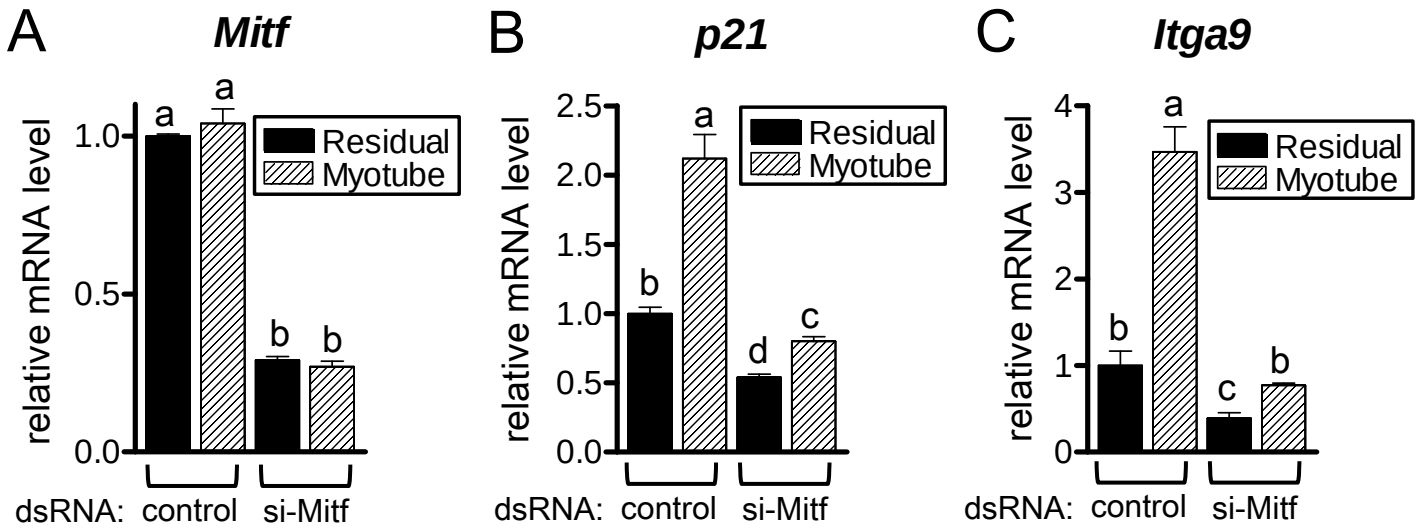
A
Mitf
relative mRNA level
1.0
0.5
0.0
a
a
b
b
Residual
Myotube
dsRNA: control si-Mitf
B
p21
relative mRNA level
2.5
2.0
1.5
1.0
0.5
0.0
b
a
d
c
Residual
Myotube
dsRNA: control si-Mitf
C
Itga9
relative mRNA level
4
3
2
1
0
b
a
c
b
Residual
Myotube
dsRNA: control si-Mitf

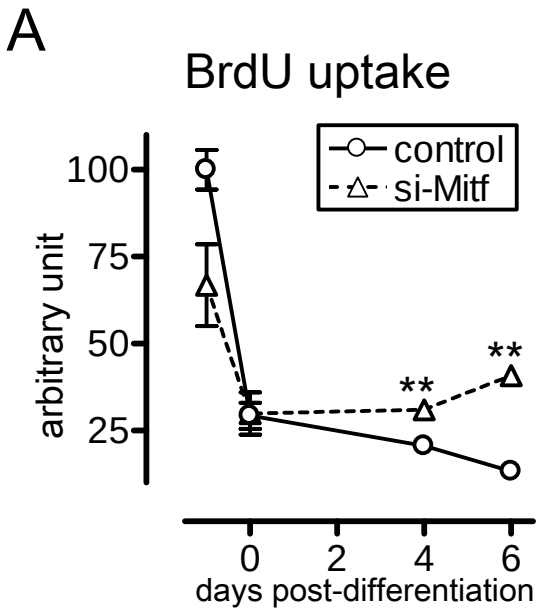
A
BrdU uptake
control
si-Mitf
arbitrary unit
100
75
50
25
**
**
0
2
4
6
days post-differentiation

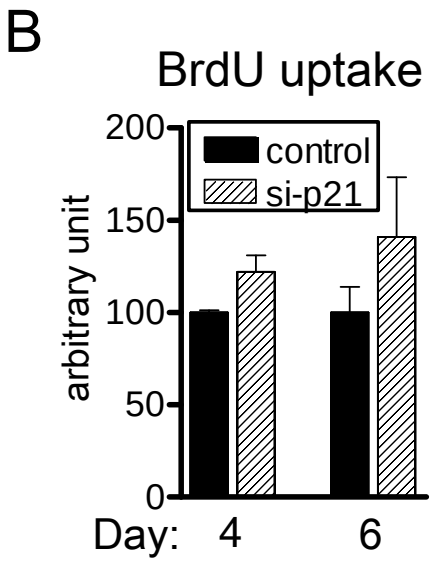
B
BrdU uptake
control
si-p21
arbitrary unit
200
150
100
50
0
Day: 4
6

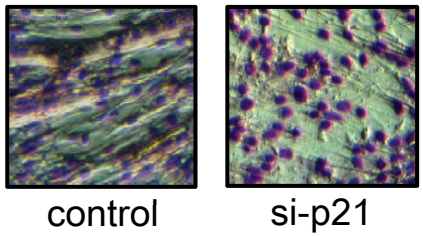
C
control
si-p21

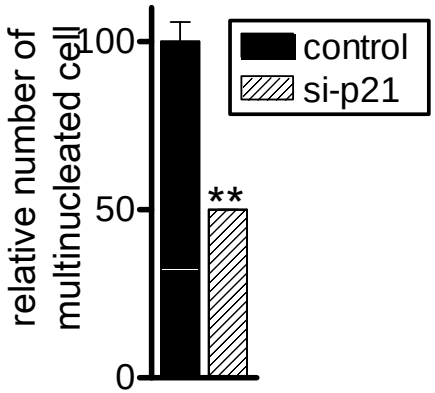
D
relative number of multinucleated cell
100
50
0
control
si-p21
**

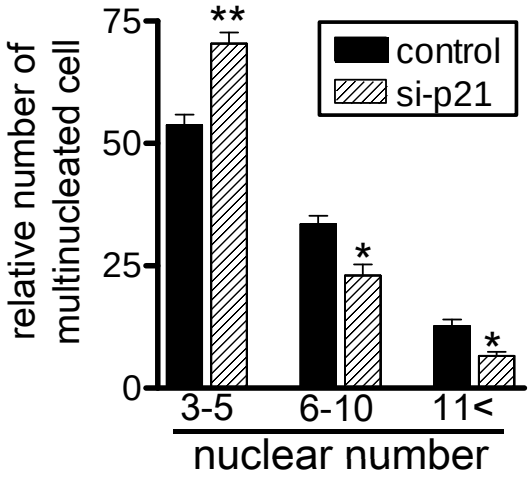
E
relative number of multinucleated cell
75
50
25
0
**
*
*
control
si-p21
3-5
6-10
11<
nuclear number

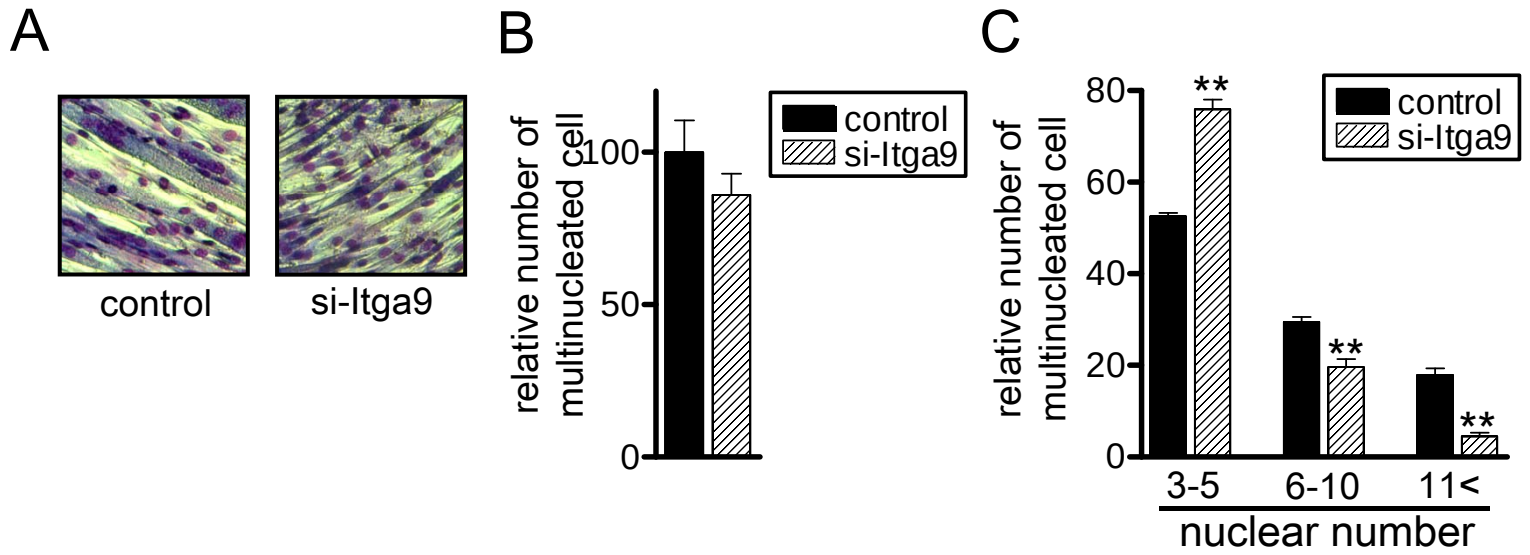
A
control
si-Itga9
B
relative number of multinucleated cell
100
50
0
control
si-Itga9
C
relative number of multinucleated cell
80
60
40
20
0
**
**
**
control
si-Itga9
3-5
6-10
11<
nuclear number

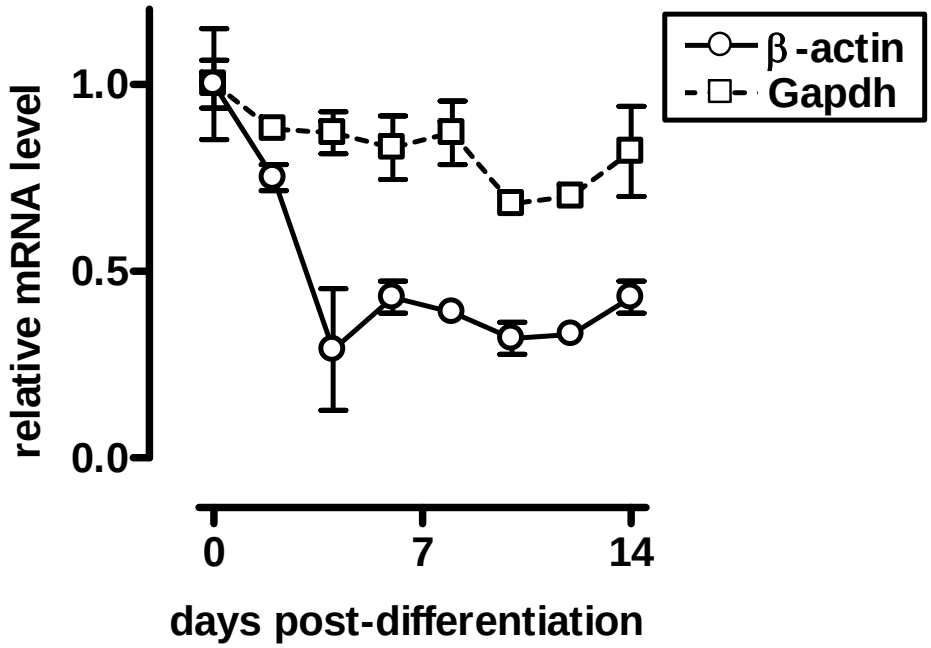
β-actin
Gapdh
relative mRNA level
1.0
0.5
0.0
0
7
14
days post-differentiation

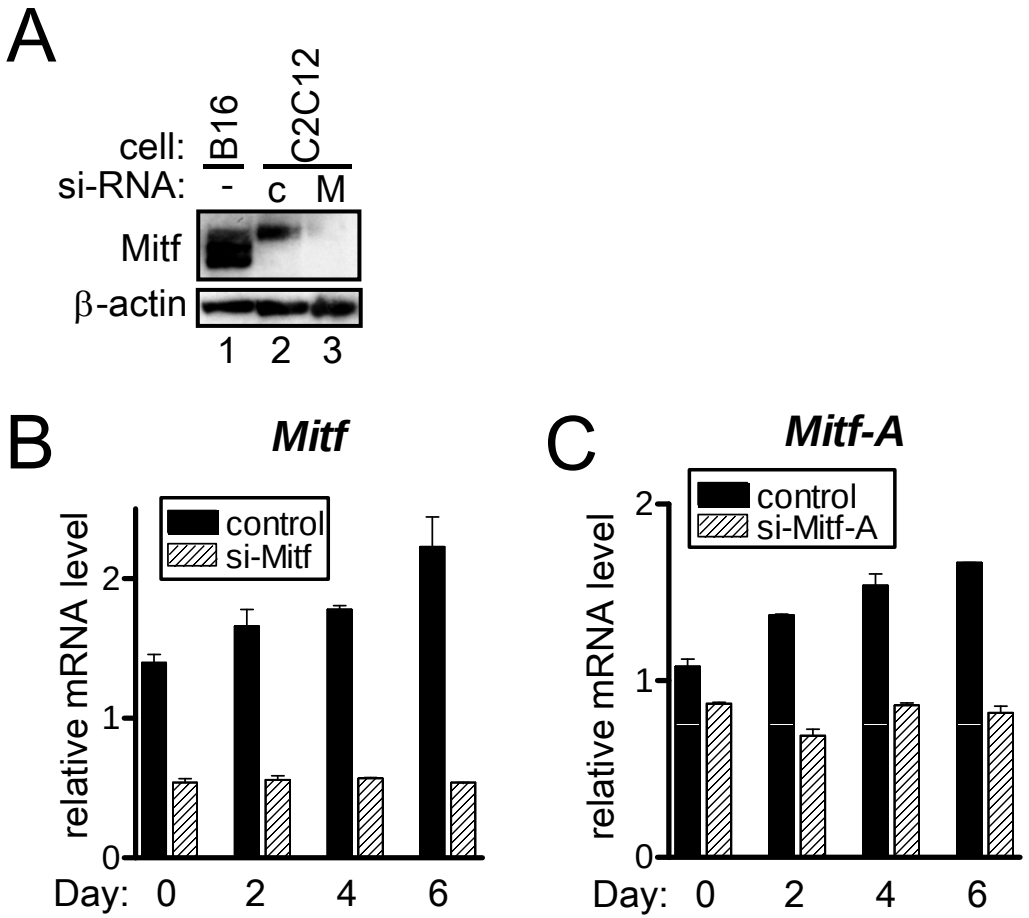
A
cell:
B16
C2C12
si-RNA:
-
c
M
Mitf
β-actin
1 2 3
B
Mitf
control
si-Mitf
relative mRNA level
0
1
2
Day: 0 2 4 6
C
Mitf-A
control
si-Mitf-A
relative mRNA level
0
1
2
Day: 0 2 4 6

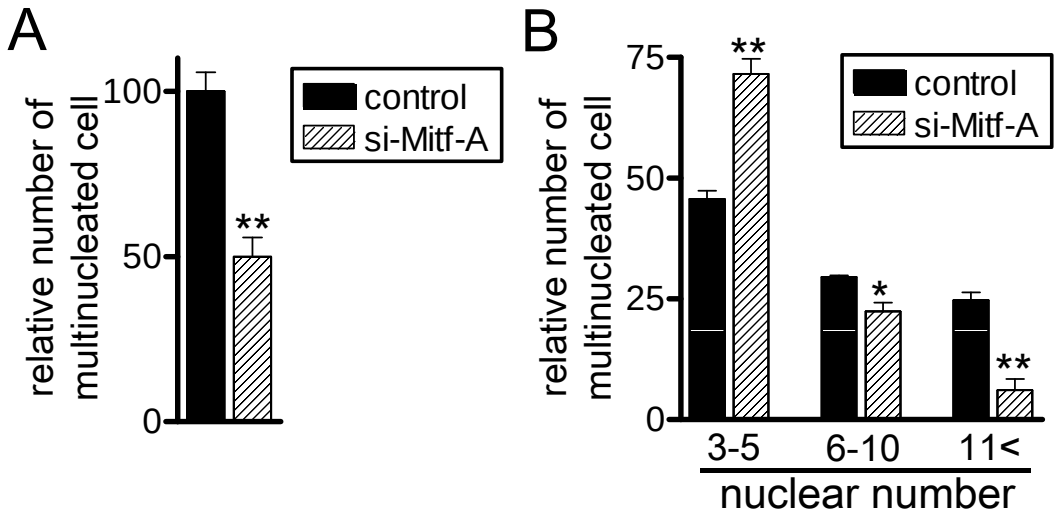
A
relative number of multinucleated cell
100
50
0
**
control
si-Mitf-A
B
relative number of multinucleated cell
75
50
25
0
**
*
**
3-5
6-10
11<
nuclear number
control
si-Mitf-A

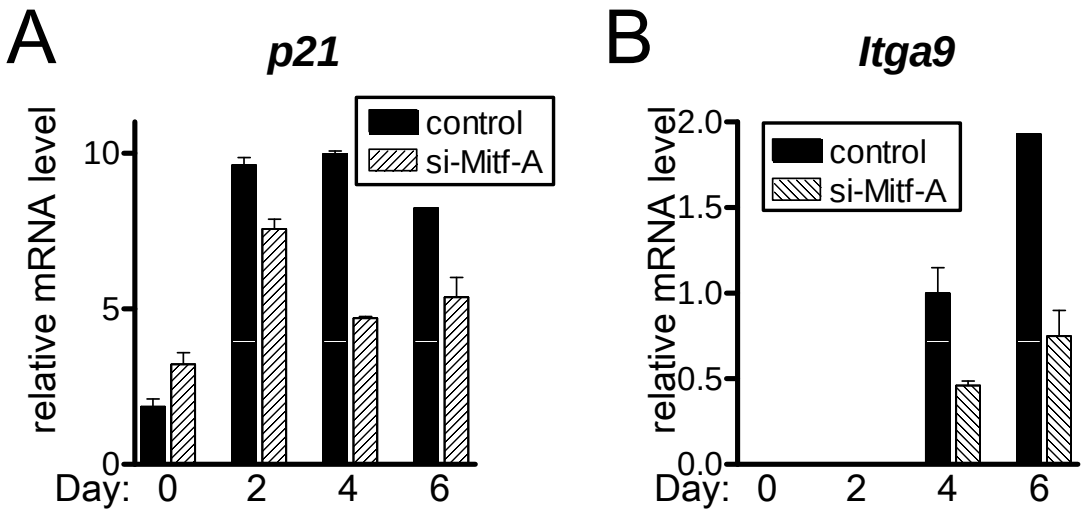
A
p21
relative mRNA level
control
si-Mitf-A
10
5
0
Day: 0 2 4 6
B
Itga9
relative mRNA level
control
si-Mitf-A
2.0
1.5
1.0
0.5
0.0
Day: 0 2 4 6

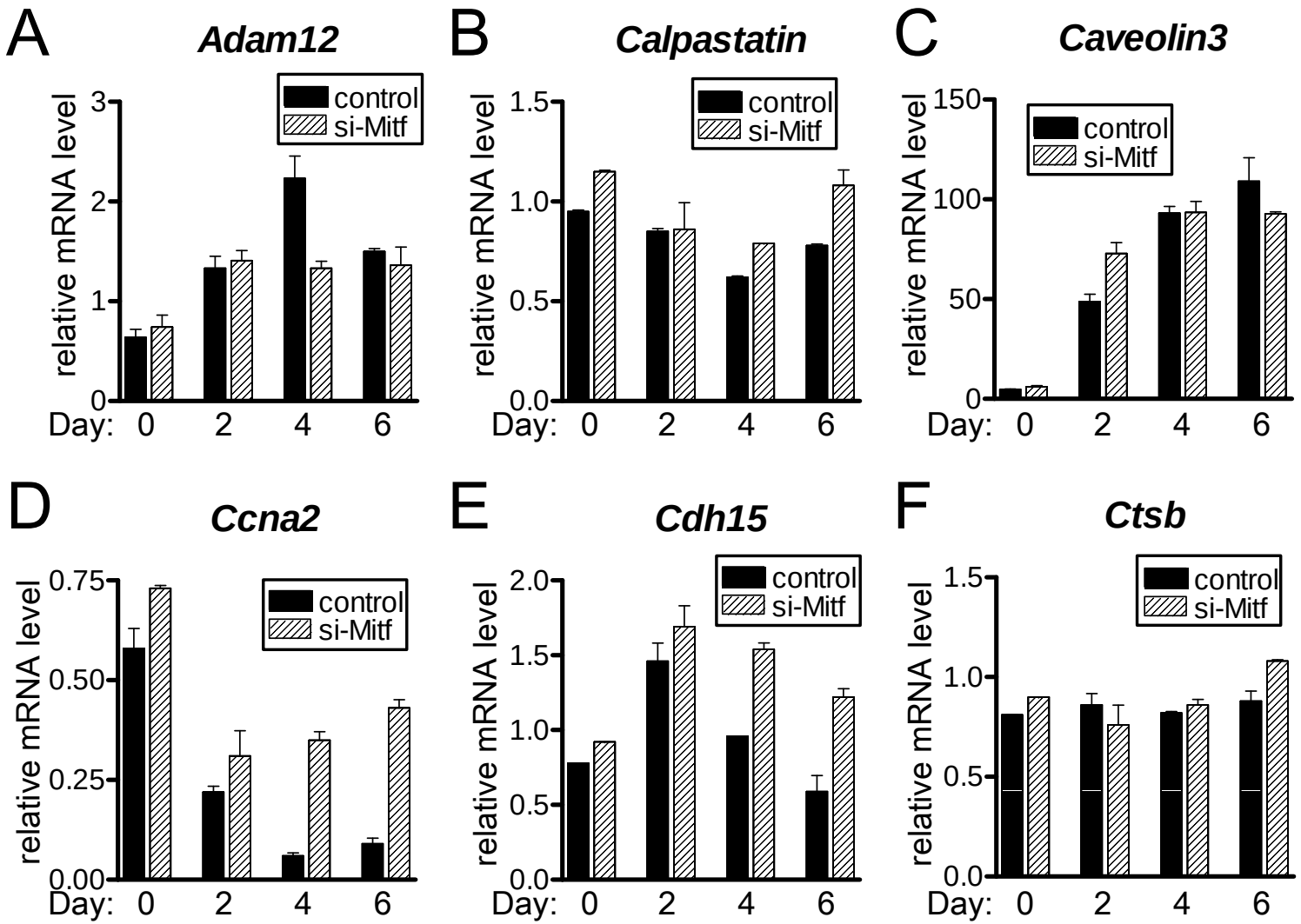
A
Adam12
B
Calpastatin
C
Caveolin3
D
Ccna2
E
Cdh15
F
Ctsb
control
si-Mitf
relative mRNA level
Day: 0 2 4 6

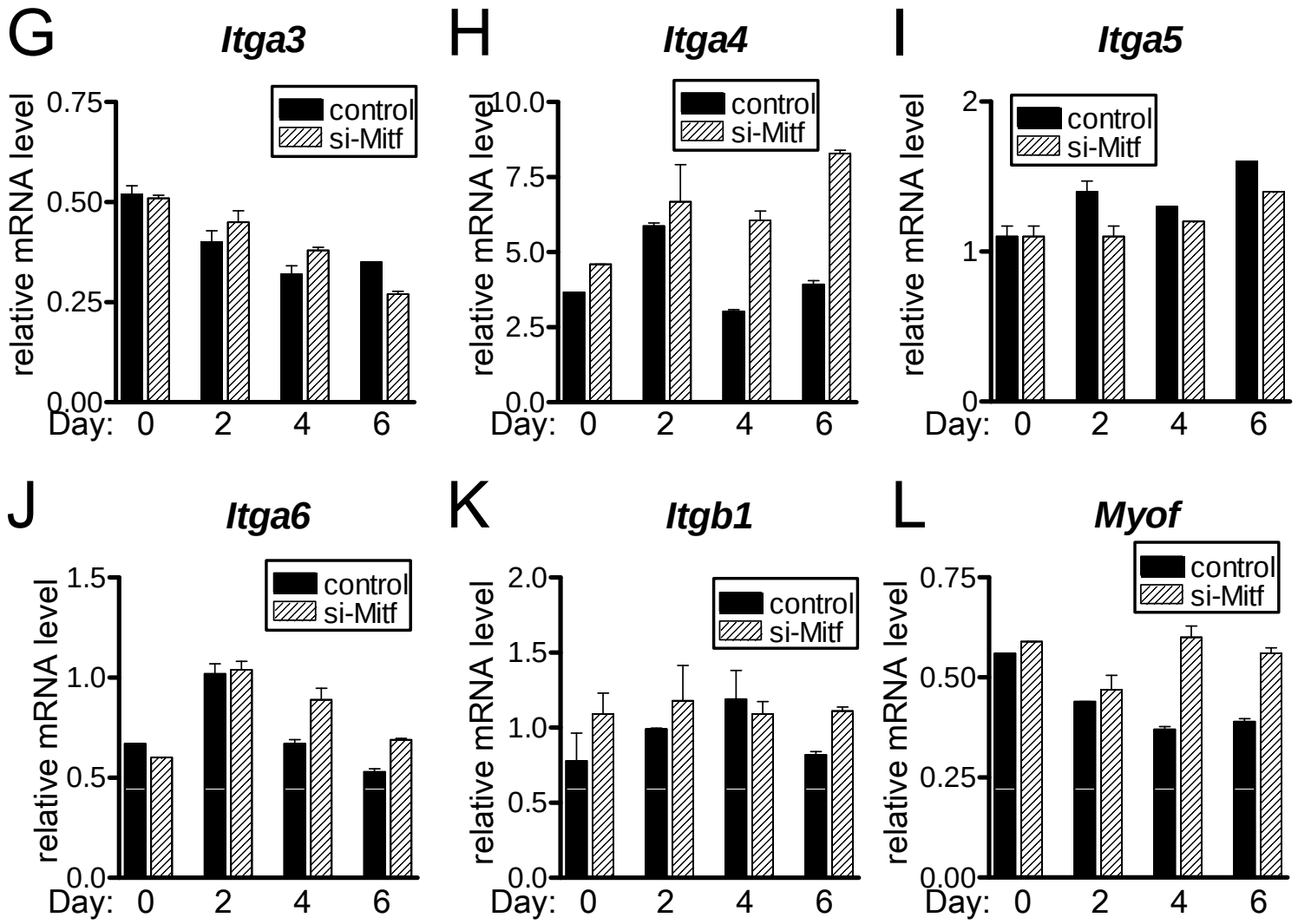
G
Itga3
H
Itga4
I
Itga5
J
Itga6
K
Itgb1
L
Myof
relative mRNA level
control
si-Mitf
Day: 0 2 4 6
0.00
0.25
0.50
0.75
0.0
2.5
5.0
7.5
10.0
0
1
2
0.5
1.0
1.5
2.0

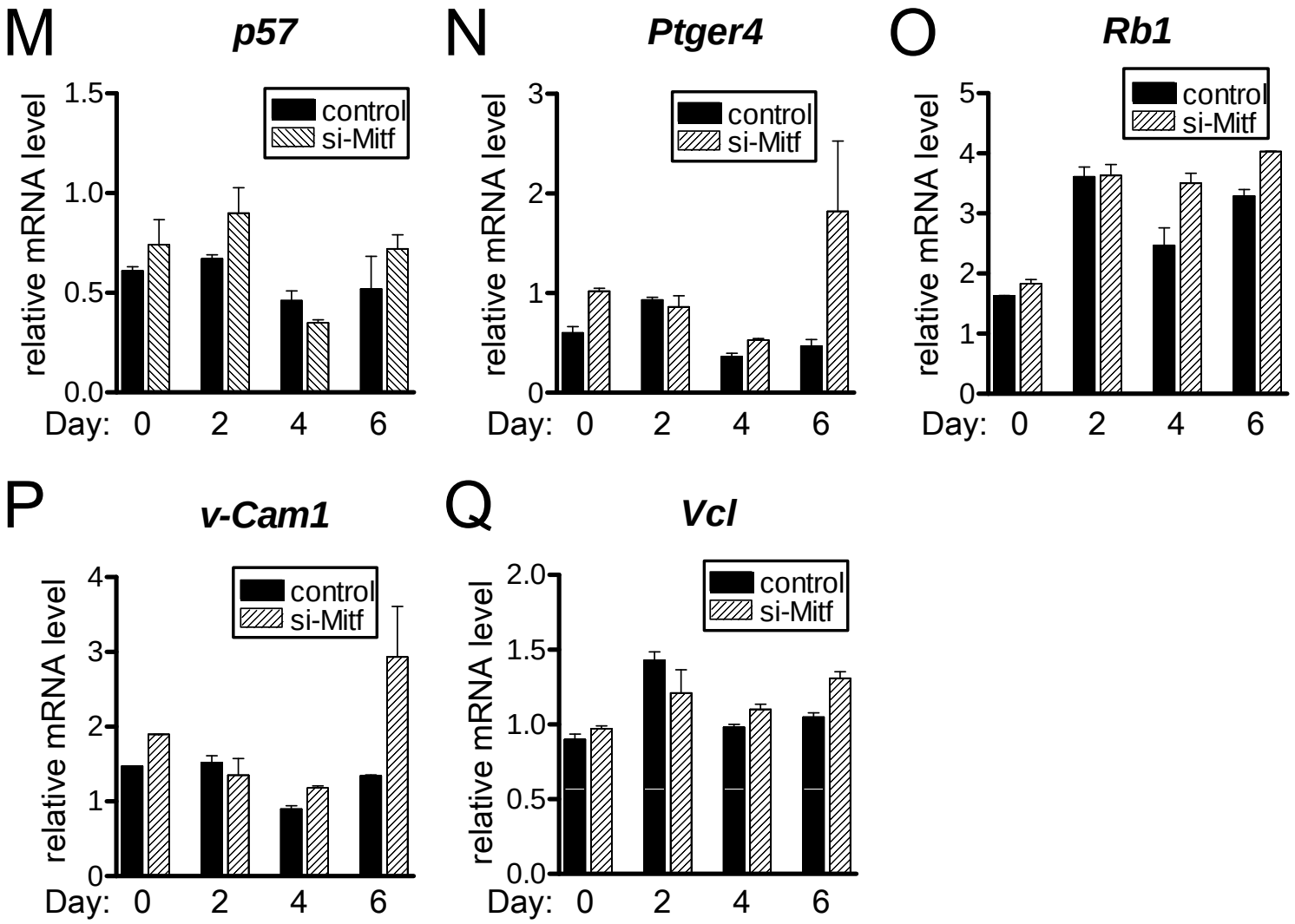
M
p57
N
Ptger4
O
Rb1
P
v-Cam1
Q
Vcl
relative mRNA level
control
si-Mitf
Day: 0 2 4 6

Table 1. Oligonucleotide PCR primers for qRT-PCR

	Oligonucleotide		GenBank
	5'-primer	3'-primer	accession number
Mitf:			
Common *Mitf*	5'-GCCTTGCAAATGGCAAATAC-3'	5'-GCTGGACAGGAGTTGCTGAT-3'	
Mitf-A	5'-GAGGAGTTTCACGAAGAACC-3'	5'-GCTGGCGTAGCAAGATGCGTGA-3'	NM_001113198
Mitf-H	5'-GAGGAGTTTCACGAAGAACC-3'	5'-GCTGGCGTAGCAAGATGCGTGA-3'	NM_001178049
Mitf-J	5'-CCGTGTCTCTGGGCATCTGAAG-3'	5'-GCTGGCGTAGCAAGATGCGTGA-3'	AY632575
Mitf-M	5'- ATGCTGGAAATGCTAGAATACAG-3'	5'-CATACCTGGGCACTCACTCTC-3'	NM_008601
Myogenic regulatory factors:			
Myf5	5'-GCCAGTTCTCCCCTTCTGAGTA-3'	5'-TGGTCCCCAAACTCATCCTCT-3'	NM_008656
Myod1	5'-GTGGCAGCGAGCACTA-3'	5'-GGGCCGCTGTAATCCATC-3'	NM_010866
Myogenin	5'-AGAAGCGCAGGCTCAAGAAA-3'	5'-ATCTCCACTTTAGGCAGCCG-3'	NM_031189
Mrf4	5'-GGGCCTCGTGATAACTGCT-3'	5'-AAGAAAGGCGCTGAAGACTG-3'	NM_008657
Myosin heavy chains:			
Myhc2a	5'-AAAGCTCCAAGGACCCTCTT-3'	5'-AGCTCATGACTGCTGAACTCAC-3'	NM_ 001039545
Myhc2b	5'-CCGAGCAAGAGCTACTGGA-3'	5'-TGTTGATGAGGCTGGTGTTC-3'	NM_010855
Myhc2x	5'-TCGCTGGCTTTGAGATCTTT-3'	5'-CGAACATGTGGTGGTTGAAG-3'	NM_ 030679
Target candidates:			
Adam12	5'-CAGAGCATCCCAGCCAAG-3'	5'-CAGGCTGAGGATCAGGTCTC-3'	NM_007400
Calpastatin	5'-CCTTCAGCTGGTGGAGAGAG-3'	5'-GCTGGTGTGAATGGTTTCTG-3'	NM_009817
Caveolin3	5'-CACAAGGCTCTGATCGCCTC-3'	5'-TCCGTGTGCTCTTCGGTCA-3'	NM_007617
Ccna2	5'-CTTGGCTGCACCAACAGTAA-3'	5'-CAAACTCAGTTCTCCCAAAAACA-3'	NM_009828
Cdh15	5'-TGACATTGCCAACTTCATCAG-3'	5'-GATGAGAGCTGTGTCGTAGGGAG-3'	NM_007662
Ctsb	5'-AAGCTGTGTGGCACTGTCCTG-3'	5'-GATCTATGTCCTCACCGAACGC-3'	NM_007798
Itga3	5'-CATCAACATGGAGAACAAGACC-3'	5'-CCAACCACAGCTCAATCTCA-3'	NM_013565

Itga4	5'-ACCAGACCTGCGAACAGC-3'	5'-CCCCCAGCCACTGGTTAT-3'	NM_010576
Itga5	5'-TACTCTGTGGCTGTGGGTGA-3'	5'-GCCATTAAGGACGGTGACAT-3'	NM_010577
Itga6	5'-GGTTGAGAGGCCATGAAAAG-3'	5'-TTCTTTTGTTCTACACGGACGA-3'	NM_008397
Itga9	5'-TGATGCCAACGTGTCCTTTA-3'	5'-GAAATGCCCATCTCCTCCT-3'	NM_133721
Itgb1	5'-ATGCAGGTTGCGGTTTGT-3'	5'-CATCCGTGGAAAACACCAG-3'	NM_010578
Myof	5'-CATTACTGGCTTCTAAGCTGTCG-3'	5'-AAATTTACTCCACCAGTCAACG-3'	NM_001099634
p21	5'-TGGGCCCGGAACATCTC-3'	5'-TGCGCTTGGAGTGATAGAAA-3'	NM_007669
p57	5'-CAGGACGAGAATCAAGAGCA-3'	5'-TGCGCTTGGCGAAGAAGT-3'	NM_009876
Ptger4	5'-TCCAGATGGTCATCTTACTCAT-3'	5'-TAACTGGTTAATGAACACTCGCA-3'	NM_001136079
Rb1	5'-GCTGCAAATACAGAGACACAAGCAG-3'	5'-CGGAGATATGCTAGACGGTACACTT-3'	NM_009029
v-Cam1	5'-TGATTGGGAGAGACAAAGCA-3'	5'-AACAACCGAATCCCCAACT-3'	NM_011693
Vcl	5'-GATAGCTGCTCTGACCTCTAA-3'	5'-TAGTGCCGTCGCCACTTGTTT-3'	NM_009502
Reference genes:			
β-actin	5'-CTAAGGCCAACCGTGAAAAG-3'	5'-ACCAGAGGCATACAGGGACA-3'	X03672
Gapdh	5'-CGTGTTCCTACCCCCAATGT-3'	5'-TGTCATCATACTTGGCAGGTTTCT-3'	NM_008084